



Synthesis, crystal structure, anticancer and molecular docking studies of quinolinone-thiazolidinone hybrid molecules

Vasanth Kumar¹ · Vaishali M. Rai² · Vishwanatha Udupi³ · Naveen Shivalingegowda⁴ · Vinitha R. Pai⁵ · Lokanath Neratur Krishnappagowda⁶ · Boja Poojary⁷

Received: 24 March 2021 / Accepted: 11 July 2021
© Iranian Chemical Society 2021

Abstract

A new series of quinolone-thiazolidinone hybrid molecules **8a-o** were prepared. Quinoline compounds were synthesized by Meth-Cohn synthesis and were condensed with 2,3-disubstituted thiazolidinone. These molecules were screened for their anticancer activities against MDA-MB-231 and MCF-7 cell line using MTT assay. Potent compounds were tested for their cytotoxicity on normal HEK 293 cell lines and most potent compound was tested for its cell cycle analysis. Molecular docking and molecular dynamic studies were performed on human N-acetyl transferase (hNAT-1) protein using Schrodinger molecular docking toolkit. Compound **8n** emerged as potent with IC₅₀ 8.16 μM against MDA-MB-231 cell line followed by **8e** with IC₅₀ 17.68 μM. Compound **8n** arrested cell cycle at G2/M phase and was non-toxic to human normal kidney cell line. The potent compound **8n** binds well with human NAT-1 protein with remarkable hydrogen bonding and π-π interactions. Molecular dynamic studies of **8n** further confirm the target for these molecules. Target quinolinone-thiazolidinones were found to be new class of compounds targeting hNAT-1 and can serve as new lead compounds in drug discovery.

Keywords Quinolinone · Thiazolidinone · Anticancer activity · hNAT-1 inhibitor · Docking studies

Introduction

Cancer is a serious health issue in both developed and developing countries causing the death of several millions of people [1, 2]. A recent survey reported that there will be five-fold increase in the cancer cases by 2025. Since, cancer spreads from organ to organ by a process called metastasis rendering treatment ineffective. Among the various types of cancer, breast cancer is responsible for increased death. Since breast tissues are prone to be attacked by cancer very rapidly. An estimated 2.3 million women were diagnosed with breast cancer therapy in 2020 across the world. In India, breast cancer remains as life threatening disease and millions of women are undergoing treatment every year. It is common in the women aged above 40 years and also in the age group of 20–30. The main problem lies in the identification of breast cancer in the early stages, thus complicating the treatment in later stages. Therefore, search of new class of anticancer agent still remains as an important area of research in the medicinal chemistry field.

Quinolinone is the important class of heterocyclic motif found in several natural products. Quinoline derivatives are reported to possess antimicrobial [3], antituberculosis [4],

✉ Boja Poojary
bojapoojary@gmail.com

- ¹ PG Department of Chemistry, Sri Dharmasthala Manjunatheshwara College (Autonomous), Ujire, India 574240
- ² Department of Microbiology, St. Aloysius College (Autonomous), Mangalore 575003, India
- ³ Department of Biotechnology and Microbiology, Sri Dharmasthala Manjunatheshwara Centre for Research in Ayurveda & Allied Sciences, Kuthpady 574118, Udupi, Karnataka, India
- ⁴ Department of Physics, Faculty of Engineering & Technology, JAIN (Deemed-to-be University), Jain Global Campus, Ramanagara Dist., Bangalore 562112, India
- ⁵ Department of Biochemistry, Yenepoya Medical College, Yenepoya University, Deralakatte, Mangalore 575018, India
- ⁶ Department of Studies in Physics, University of Mysore, Manasagangotri, Mysuru 570006, India
- ⁷ Department of Studies and Research in Chemistry, Mangalore University, Mangalagangothri, Karnataka 574199, India

anti-inflammatory [5], neuroprotective [6], antioxidant [7], and antidepressant [8] activities. Moreover, Quinolone derivatives are well known to exhibit anticancer activity [9], in particular, compound **1–3** were emerged as potent anti-tumour agent (Fig. 1) [10–12]. Hence, search of newer quinolone-based entities for their diversified pharmacological activity has gaining more focus.

Thiazolidine-4-one motifs have occupied a unique place in the medicinal chemistry and are regarded as ‘magic moiety’ which possesses most of the biological activities [13]. Due to their small size and ability to form strong binding with receptors made the researcher to synthesize library of thiazolidinone compounds [14–16]. Thiazolidinone derivatives are associated with wide range of activities such as antimicrobial [17, 18], anti-inflammatory [19, 20], antitubercular [21, 22], anti-diabetic [23, 24], antiamebic [25],

anti-HIV-1 [26], anticonvulsant [27] and HCV NS5B polymerase inhibitor [28]. In the recent years, researchers are more focussing on thiazolidinone-based small molecules in the anticancer field [29–31] as they are capable of bind properly into the active pockets of receptors. Notably, **4** showed significant CAIX inhibiting activity [32] and **5** showed excellent anticancer activity against MCF-7 breast cancer cell lines with nanomolar level of inhibition [33] (Fig. 1).

N-acetyl transferase is an emerging target in the anticancer field. In the recent years, it was evidenced from the studies that NAT1 is more expressed in cancer cells. Especially, these are expressed in breast cancer cells. Some small molecules were reported as NAT1 inhibitors like Rhodanine derivative (**6**) as a selective inhibitor of recombinant human NAT1 and inhibited the NAT activity of cell lysates of breast cancer cells ZR-75-1 [34]. Also, another rhodanine molecule (**7**) inhibited the

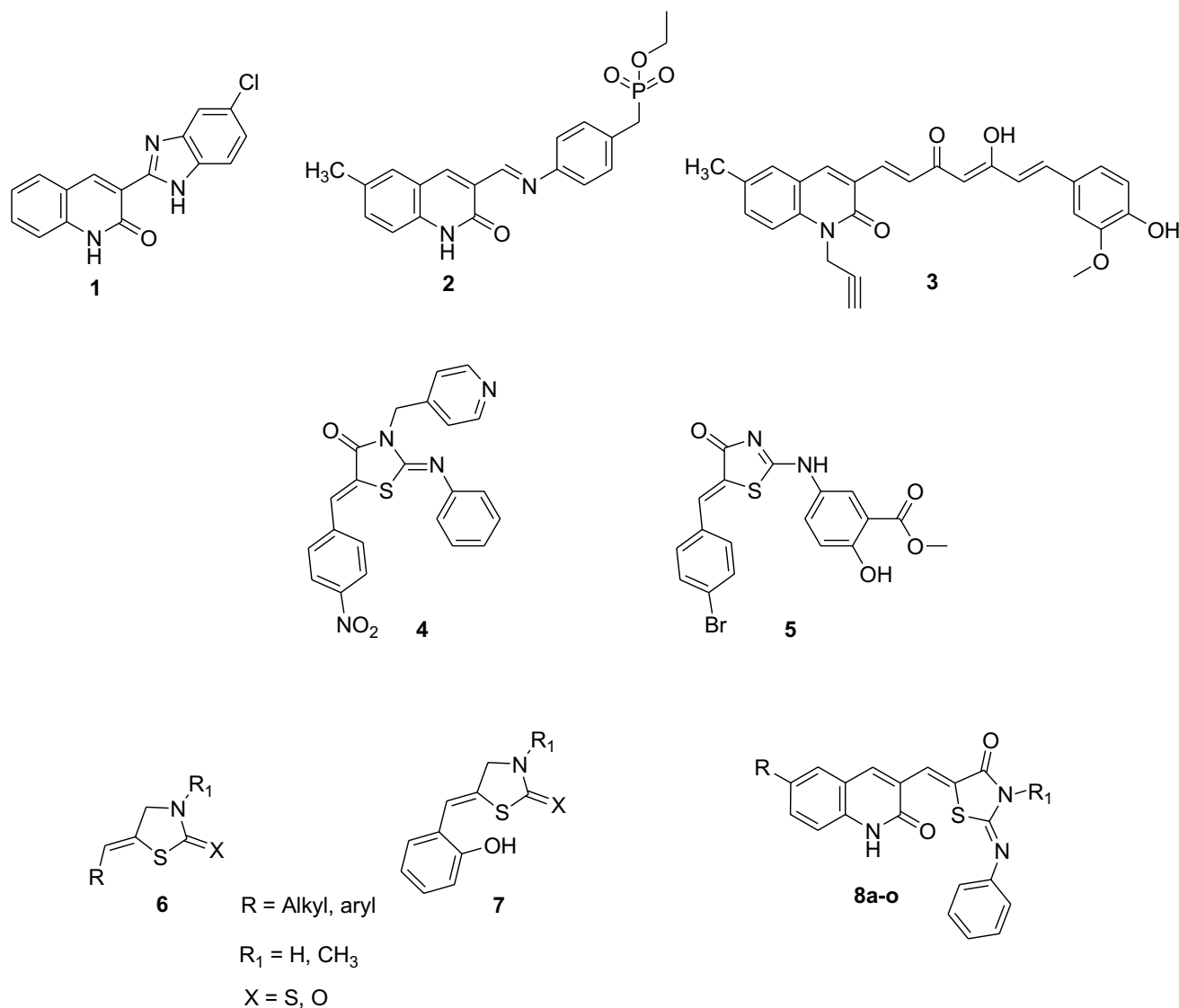


Fig. 1 Potential anticancer compounds (**1–5**), *h*NAT1 inhibitors (**6,7**) and target compounds **8a-o**

NAT1 activity in intact MDA-MB-231 cells in a concentration dependant manner. It also inhibited the proliferation by blocking the cells in G₂/M phase [35]. Recently, it was also shown that the currently using chemotherapeutic agents such as Cisplatin [36] and Tamoxifene [37, 38] inhibit the NAT1 activity. The two breast cancer cells MCF-7 and MDA-MB-231 treated with Cisplatin showed considerable NAT1 inhibition with IC₅₀ less than 100 μM. Hence, NAT1 was considered as novel target for the development of newer drug candidates.

Encouraged by the aforementioned activities of thiazolidine-4-ones and quinolones, we planned to synthesize some hybrid compounds comprising these two units. In our present study, we varied thiazolidine-4-one motif by varying substitutions attached to the nitrogen atom at 3rd position as well as by varying substituent at the 6th position of quinoline moiety. All the new compounds were initially screened for anti-breast cancer activity on MDA-MB-231 cell line and five of the potent compounds were then screened on MCF-7 breast cancer cell line by MTT assay. Further to understand the mechanism of action, cell cycle analysis was done on MDA-MB-231 cell line by flow cytometry method. Molecular docking studies were performed to understand the possible binding interactions of the molecules on human *N*-acetyl transferase (NAT-1) protein.

Experimental

General

All the starting materials were purchased from Sigma Aldrich (India). All the solvents and reagents were purchased from the commercial vendors in the appropriate grade and were used without purification. Melting points were determined by an open capillary method and are uncorrected. FTIR spectra were recorded on a Shimadzu FTIR 157 Spectrometer in KBr pellet. ¹H NMR spectra were measured on BRUKER AVANCE II-400 (300 MHz) spectrometer using TMS as an internal standard. The chemical shifts are reported in δ units and the coupling constants (J) are reported in hertz. Mass spectra were recorded in Agilent Technology LC-mass spectrometer. Elemental analyses were carried out using CHNS Elementar Vario EL III. Purity of the compounds was checked by thin layer chromatography (TLC) on a silica-coated aluminium sheet (silica gel 60F254) using ethyl acetate and hexane (3:7, v/v).

Chemistry

General procedure for the synthesis of substituted phenylthioureas (6a-c)

To a mixture of substituted amine (0.01 moles) in *N,N*-dimethylformamide (10v) added phenylisothiocyanate

(0.01 moles) and triethylamine (0.02 moles) slowly at room temperature. Reaction mixture was stirred at room temperature for 10 h. After the completion of reaction, reaction mass was quenched into crushed ice. Solid precipitated was filtered off, washed with cold water and dried.

1-(4-fluorobenzyl)-3-phenylthiourea (6c)

Yield: 85%; FTIR (KBr, cm⁻¹): 3391, 3120, 3094, 3005, 2982, 1597, 1543, 1184; ¹H NMR (400 MHz, DMSO-d₆, δ, ppm): 9.64 (s, 1H, N-H), 8.18 (s, 1H, N-H), 7.31–7.42 (m, 6H, Ar-H), 7.12–7.18 (m, 3H, Ar-H), 4.73 (s, 2H, -CH₂); ¹³C NMR (100 MHz, DMSO, δ, ppm): 181.24 (C=S), 160.49, 139.56, 135.75, 129.95, 128.87, 129.13, 128.90, 124.84, 124.11, 123.90, 115.53, 115.32, 46.89; LCMS (*m/z*): 261.15 (M+H)⁺; Anal. Calcd. For C₁₄H₁₃FN₂S: C, 64.59; H, 5.03; N, 10.76. Found: C, 64.66; H, 5.09; N, 10.70.

General procedure for the synthesis of 2-phenylimino-3-substituted-thiazolidin-4-ones (7a-c)

To the substituted phenylthiourea (0.01 moles) (6a-c) added anhydrous sodium acetate (0.025 moles) and chloroacetic acid (0.0125 moles) in absolute ethanol. Reaction mixture was refluxed for 12 h. After the completion of reaction, it was cooled. Solid precipitated was filtered off, washed with ethanol followed by water and dried.

3-(4-Fluorobenzyl)-2-(phenylimino)thiazolidin-4-one (7c)

Yield: 90%; FTIR (KBr, cm⁻¹): 3364, 3319, 3292, 3071, 3042, 2972, 1649, 1622, 1524, 822; ¹H NMR (400 MHz, CDCl₃, δ, ppm): 7.44 (t, 3H); 7.36 (t, 2H, Ar-H); 7.11–7.21 (m, 3H Ar-H), 6.91 (d, 1H, 8 Hz, Ar-H), 5.00 (s, 2H, CH₂), 4.10 (s, 2H, -CH₂); ¹³C NMR (100 MHz, DMSO, δ, ppm): 172.4 (C=O), 163.2, 155.4, 148.3, 130.5, 130.4, 129.8, 128.9, 124.8, 121.3, 115.79, 115.6, 45.1, 33.0; LCMS (*m/z*): 301.1 (M+H)⁺; Anal. Calcd. For C₁₆H₁₃FN₂OS: C, 63.98; H, 4.36; N, 9.33. Found: C, 63.94; H, 4.30; N, 9.38.

General procedure for the synthesis of (8a-o)

To a solution of 7a-c (0.01 moles), substituted 2-chloroquinoline-3-carboxaldehyde 3a-e (0.01 moles) and anhydrous sodium acetate (0.025 moles) in glacial acetic acid (20 ml) was refluxed for 10 h. After completion of the reaction, it was cooled to room temperature. Resulting

solid was filtered off, washed with water, dried and recrystallized from *N, N*-dimethyl formamide.

6-Fluoro-3-(*Z*-(*Z*-4-oxo-2-phenylimino-3-propylthiazolidin-5-ylidene)methyl)-quinoline-2(1H)-one (8a)

Yield: 90%; FTIR (KBr, cm^{-1}): 3150 (N–H), 3076 (Ar–H arom), 2968, 1697 (C=O), 1655 (O=C–N–H), 1128; ^1H NMR (400 MHz, DMSO- d_6 , δ , ppm): 12.14 (s, 1H, NH), 8.00 (s, 1H, Q- H_4), 7.83 (s, 1H, HC=), 7.70 (d, 1H, 8.4 Hz, Q- H_5), 7.40–7.45 (m, 3H, Q- H_8 & Ar–H), 7.31–7.34 (m, 1H, Q- H_7), 7.20 (t, 1H, 7.4 Hz, Ar–H), 7.03 (d, 2H, 7.2 Hz, Ar–H), 3.87 (t, 2H, 6.8 Hz, $-\text{CH}_2$), 1.77–1.72 (m, 2H, $-\text{CH}_2$), 0.94 (t, 3H, 7.2 Hz, $-\text{CH}_3$); ^{13}C NMR (100 MHz, DMSO, δ , ppm): 166.4 (C=O), 160.4 (C=O), 159.8, 150.1, 147.8 (=CH), 140.6, 134.1, 129.9, 128.4, 126.0, 125.7, 125.3, 123.4, 121.1, 119.4, 115.5, 49.7, 26.7, 11.6; LCMS (m/z): 408.1 (M+H) $^+$; Anal. Calcd. For $\text{C}_{22}\text{H}_{18}\text{FN}_3\text{O}_2\text{S}$: C, 64.85; H, 4.45; N, 10.31. Found: C, 64.80; H, 4.49; N, 10.38.

6-Chloro-3-(*Z*-(*Z*-4-oxo-2-phenylimino-3-propylthiazolidin-5-ylidene)methyl)-quinolin-2(1H)-one (8b)

Yield: 78%; FTIR (KBr, cm^{-1}): 3147 (N–H), 3072 (Ar–H arom), 2968, 1700 (C=O), 1656 (O=C–N–H), 828; ^1H NMR (400 MHz, CDCl_3 , δ , ppm): 12.12 (s, 1H, –NH); 8.03 (s, 1H, Q H_4); 7.90 (s, 1H, Q- H_5), 7.85 (s, 1H, HC=); 7.58 (d, 1H, 8 Hz, Q- H_7); 7.42 (t, 2H, 7.2 Hz, Ar–H); 7.32 (d, 1H, Q- H_8), 7.20 (t, 1H, 7.4 Hz, Ar–H), 7.03 (d, 2H, 8.4 Hz, Ar–H), 3.87 (t, 2H, 8 Hz, $-\text{CH}_2$), 1.70–1.79 (m, 2H, $-\text{CH}_2$), 0.94 (t, 3H, 8 Hz, $-\text{CH}_3$); ^{13}C NMR (100 MHz, DMSO, δ , ppm): 166.5 (C=O), 160.2, 150.3, 147.5 (=CH), 140.2, 134.0, 132.6, 129.8, 128.5, 126.0, 125.6, 125.2, 123.6, 120.9, 119.9, 116.5, 49.8, 26.7, 11.5; LCMS (m/z): 425.0 (M+H) $^+$; Anal. Calcd. For $\text{C}_{22}\text{H}_{18}\text{ClN}_3\text{O}_2\text{S}$: C, 62.33; H, 4.28; N, 9.91. Found: C, 62.37; H, 4.24; N, 9.96.

6-Bromo-3-(*Z*-(*Z*-4-oxo-2-(phenylimino)-3-propylthiazolidin-5-ylidene)methyl)-quinolin-2(1H)-one (8c)

Yield: 72%; FTIR (KBr, cm^{-1}): 3152 (N–H), 3070, 2966, 1702 (C=O), 1654; ^1H NMR (400 MHz, DMSO- d_6 , δ , ppm): 12.10 (s, 1H, –NH); 8.07 (s, 1H, Q- H_4); 8.01 (s, 1H, Q- H_5); 7.84 (s, 1H, HC=); 7.654 (d, 1H, 8 Hz, Q- H_8); 7.42 (t, 2H, 7.2 Hz, Ar–H); 7.28 (d, 1H, 8 Hz, Q- H_7), 7.21 (t, 1H, Ar–H, 7.6 Hz), 7.01 (d, 2H, 8 Hz, Ar–H), 3.86 (t, 2H, 8 Hz, $-\text{CH}_2$), 1.70–1.76 (m, 2H, $-\text{CH}_2$), 0.95 (t, 3H, 8 Hz, $-\text{CH}_3$); ^{13}C NMR (100 MHz, DMSO, δ , ppm): 166.5 (C=O), 160.0, 150.1, 147.9 (=CH), 140.0, 137.2, 134.0, 132.2, 130.0, 128.4, 125.9, 125.5, 125.2, 123.4, 121.0, 119.2, 115.6, 49.8, 26.5, 11.7; LCMS (m/z): 469.6 (M+H) $^+$; Anal. Calcd. For $\text{C}_{22}\text{H}_{18}\text{BrN}_3\text{O}_2\text{S}$: C, 56.42; H, 3.87; N, 8.97. Found: C, 56.47; H, 3.83; N, 8.93.

6-Methyl-3-(*Z*-(*Z*-4-oxo-2-phenylimino-3-propylthiazolidin-5-ylidene)methyl)-quinolin-2(1H)-one (8d)

Yield: 71%; FTIR (KBr, cm^{-1}): 3164, 3078, 2975, 1705, 1658, 1524; ^1H NMR (400 MHz, DMSO- d_6 , δ , ppm): 12.13 (s, 1H, –NH); 7.98 (s, 1H, Q- H_4); 7.82 (s, 1H, HC=); 7.56 (s, 1H, Q- H_5); 7.41 (t, 2H, 7.4 Hz, Ar–H); 7.34 (d, 1H, 8 Hz, Q- H_7), 7.25–7.20 (m, 2H, Q- H_7 & Ar–H); 7.02 (d, 2H, 8 Hz, Ar–H), 3.87 (t, 2H, 8 Hz, $-\text{CH}_2$); 2.30 (s, 3H, $-\text{CH}_3$); 1.71–1.78 (m, 2H, $-\text{CH}_2$), 0.94 (t, 3H, 8 Hz, $-\text{CH}_3$); ^{13}C NMR (100 MHz, DMSO, δ , ppm): 166.6 (C=O), 160.1, 150.4, 147.4 (=CH), 140.0, 136.5, 134.1, 132.0, 130.0, 128.5, 126.0, 125.6, 125.3, 123.5, 121.2, 119.4, 115.5, 49.7, 26.6, 11.7; LCMS (m/z): 404.5 (M+H) $^+$; Anal. Calcd. For $\text{C}_{23}\text{H}_{21}\text{N}_3\text{O}_2\text{S}$: C, 68.46; H, 5.25; N, 10.41. Found: C, 68.50; H, 5.29; N, 10.37.

6-Methoxy-3-(*Z*-(*Z*-4-oxo-2-phenylimino-3-propylthiazolidin-5-ylidene)methyl)-quinolin-2(1H)-one (8e)

Yield: 76%; FTIR (KBr, cm^{-1}): 3162, 3064, 2960, 1704, 1654, 1535; ^1H NMR (400 MHz, DMSO- d_6 , δ , ppm): 12.00 (s, 1H, –OH); 8.01 (s, 1H, Q- H_4); 7.85 (s, 1H, HC=); 7.42–7.44 (t, 2H, 8 Hz, Ar–H); 7.32 (s, 1H, Q- H_5); 7.28 (d, 1H, 7.6 Hz, Q- H_7), 7.25 (d, 1H, 7.2 Hz, Q- H_8), 7.21 (t, 1H, Ar–H); 7.01 (d, 2H, 8 Hz, Ar–H), 3.86 (t, 2H, 8 Hz, $-\text{CH}_2$); 3.75 (s, 3H, $-\text{CH}_3$); 1.69–1.79 (m, 2H, $-\text{CH}_2$), 0.93 (t, 3H, 8 Hz, $-\text{CH}_3$); ^{13}C NMR (100 MHz, DMSO, δ , ppm): 166.6 (C=O), 160.0, 154.5, 150.0, 147.9 (=CH), 140.5, 134.0, 130.0, 126.0, 125.7, 125.4, 123.5, 122.2, 121.25, 120.0, 116.9, 110.2, 49.7, 26.6, 11.7; LCMS (m/z): 420.2 (M+H) $^+$; Anal. Calcd. For $\text{C}_{23}\text{H}_{21}\text{N}_3\text{O}_3\text{S}$: C, 65.85; H, 5.05; N, 10.02. Found: C, 65.81; H, 5.10; N, 10.06.

3-(*Z*-(*Z*-3-Benzyl-4-oxo-2-(phenylimino)thiazolidin-5-ylidene)methyl)-6-fluoro-quinolin-2(1H)-one (8f)

Yield: 68%; FTIR (KBr, cm^{-1}): 3147, 3039, 2980, 1709, 1652, 1085; ^1H NMR (400 MHz, DMSO- d_6 , δ , ppm): 12.00 (s, 1H, –OH); 8.01 (s, 1H, Q- H_4); 7.85 (s, 1H, HC=); 7.71 (d, 1H, 7.6 Hz, Q- H_5), 7.47–7.40 (m, 8H, Ar–H, Q- H_8); 7.35–7.30 (m, 1H, Q- H_7); 7.21 (t, 1H, Ar–H); 7.01 (d, 2H, 8 Hz, Ar–H), 5.10 (s, 2H, $-\text{CH}_2$); ^{13}C NMR (100 MHz, DMSO, δ , ppm): 166.3, 160.9, 160.0, 151.0, 148.0 (=CH), 141.0, 133.9, 132.2, 129.8, 129.0, 128.7, 128.5, 128.1, 127.9, 125.9, 125.6, 125.2, 123.0, 121.1, 119.6, 115.2, 46.4, 31.1; LCMS (m/z): 456.3 (M+H) $^+$; Anal. Calcd. For $\text{C}_{26}\text{H}_{18}\text{FN}_3\text{O}_2\text{S}$: C, 68.56; H, 3.98; N, 9.22. Found: C, 68.48; H, 3.93; N, 9.27.

3-(Z-(Z-3-benzyl-4-oxo-2-(phenylimino)thiazolidin-5-ylidene)methyl)-6-chloro-quinolin-2(1H)-one (8 g)

Yield: 90%; FTIR (KBr, cm^{-1}): 3151, 3045, 2972, 1704, 1650, 844; ^1H NMR (400 MHz, DMSO-d_6 , δ , ppm): 12.00 (s, 1H, -OH); 8.00 (s, 1H, Q-H₄), 7.93 (s, 1H, Q-H₅), 7.84 (s, 1H, HC=); 7.62 (d, 1H, 8 Hz, Q-H₇); 7.37–7.45 (m, 6H, Ar-H); 7.31 (d, 1H, Q-H₈); 7.21 (t, 1H, Ar-H); 7.02 (d, 2H, 8 Hz, Ar-H), 5.09 (s, 2H, -CH₂); ^{13}C NMR (100 MHz, DMSO , δ , ppm): 166.4, 160.2, 150.9, 147.8 (=CH), 140.8, 134.0, 132.0, 130.0, 129.1, 128.9, 128.3, 128.1, 128.8, 126.0, 125.8, 125.4, 123.4, 121.3, 120.4, 116.8, 46.6, 31.0; LCMS (m/z): 473.0 (M+H)⁺; Anal. Calcd. For $\text{C}_{26}\text{H}_{18}\text{ClN}_3\text{O}_2\text{S}$: C, 66.17; H, 3.84; N, 8.90. Found: C, 66.22; H, 3.81; N, 8.96.

3-(Z-(Z-3-benzyl-4-oxo-2-(phenylimino)thiazolidin-5-ylidene)methyl)-6-bromo-quinolin-2(1H)-one (8 h)

Yield: 74%; FTIR (KBr, cm^{-1}): 3154, 3045, 2978, 1702, 1651, 1580; ^1H NMR (400 MHz, DMSO-d_6 , δ , ppm): 12.01 (s, 1H, -OH); 8.07 (s, 1H, Q-H₄); 8.00 (s, 1H, Q-H₅); 7.82 (s, 1H, HC=); 7.63 (d, 1H, 8 Hz, Q-H₈); 7.37–7.47 (m, 7H, Ar-H); 7.30 (d, 1H, 7.6 Hz, Q-H₇), 7.20 (t, 1H, 7.4 Hz, Ar-H), 7.02 (d, 2H, Ar-H); 5.07 (s, 2H, -CH₂); ^{13}C NMR (100 MHz, DMSO , δ , ppm): 166.8, 161.0, 151.2, 148.0 (=CH), 141.3, 137.5, 131.8, 134.2, 132.3, 129.9, 129.0, 128.8, 128.2, 127.9, 125.9, 125.7, 125.3, 123.5, 121.2, 120.0, 116.0, 46.3, 31.1; LCMS (m/z): 517.6 (M+H)⁺; Anal. Calcd. For $\text{C}_{26}\text{H}_{18}\text{BrN}_3\text{O}_2\text{S}$: C, 60.47; H, 3.51; N, 8.14. Found: C, 60.42; H, 3.56; N, 8.10.

3-(Z-(Z-3-benzyl-4-oxo-2-(phenylimino)thiazolidin-5-ylidene)methyl)-6-methyl-quinolin-2(1H)-one (8i)

Yield: 74%; FTIR (KBr, cm^{-1}): 3150, 3034, 2986, 1705, 1651, 1589; ^1H NMR (400 MHz, DMSO-d_6 , δ , ppm): 12.00 (s, 1H, -OH); 7.97 (s, 1H, Q-H₄); 7.85 (s, 1H, HC=); 7.55 (s, 1H, Q-H₅), 7.36–7.43 (m, 7H, Ar-H); 7.32 (d, 1H, 8 Hz, Q-H₇); 7.20 (t, 2H, Q-H₈, Ar-H); 7.00 (d, 2H, Ar-H); 5.10 (s, 2H, -CH₂); 2.31 (s, 3H, -CH₃); ^{13}C NMR (100 MHz, DMSO , δ , ppm): 166.4, 160.8, 150.6, 148.0 (=CH), 141.0, 137.3, 136.3, 133.4, 132.1, 130.0, 129.0, 128.9, 128.1, 128.0, 126.0, 125.7, 125.3, 123.2, 121.4, 119.4, 115.5, 46.2, 31.1; LCMS (m/z): 452.3 (M+H)⁺; Anal. Calcd. For $\text{C}_{27}\text{H}_{21}\text{N}_3\text{O}_2\text{S}$: C, 71.82; H, 4.69; N, 9.31. Found: C, 71.78; H, 4.75; N, 9.35.

3-(Z-(Z-3-benzyl-4-oxo-2-(phenylimino)thiazolidin-5-ylidene)methyl)-6-methoxy-quinolin-2(1H)-one (8j)

Yield: 74%; FTIR (KBr, cm^{-1}): 3147, 3042, 2980, 1703, 1654, 1580; ^1H NMR (400 MHz, DMSO-d_6 , δ , ppm): 12.01 (s, 1H, -NH); 7.98 (s, 1H, Q-H₄); 7.84 (s, 1H, HC=); 7.37–7.44 (m, 7H, Ar-H); 7.33 (s, 1H, Q-H₅); 7.28 (d, 1H, 7.6 Hz, Q-H₇), 7.25–7.20 (m, 2H, Q-H₈, Ar-H); 7.02 (d, 2H, Ar-H); 5.09 (s, 2H, -CH₂); 3.76 (s, 3H, -OCH₃); ^{13}C NMR (100 MHz, DMSO , δ , ppm): 166.9, 161.0, 154.8, 150.7, 147.8 (=CH), 140.7, 134.1, 132.0, 130.0, 129.1, 128.5, 128.0, 126.1, 125.8, 125.6, 123.8, 122.3, 121.0, 120.0, 116.6, 110.2, 46.4, 31.2; LCMS (m/z): (M+H)⁺ 468.5; Anal. Calcd. For $\text{C}_{27}\text{H}_{21}\text{N}_3\text{O}_3\text{S}$: C, 69.36; H, 4.53; N, 8.99. Found: C, 69.32; H, 4.58; N, 8.95.

3-(Z-(Z-3-(4-fluorophenyl)-4-oxo-2-(phenylimino)thiazolidin-5-ylidene)methyl)-6-fluoro-quinolin-2(1H)-one (8 k)

Yield: 68%; FTIR (KBr, cm^{-1}): 3222, 3071, 2975, 1712, 1653, 1582, 1184; ^1H NMR (400 MHz, DMSO-d_6 , δ , ppm): 12.00 (s, 1H, -OH); 8.01 (s, 1H, Q-H₄); 7.85 (s, 1H, HC=); 7.72 (d, 1H, Q-H₅); 7.48–7.42 (m, 4H, Ar-H, Q-H₇, Q-H₈); 7.21 (t, 1H, Ar-H); 7.01 (d, 2H, 8 Hz, Ar-H), 5.02 (s, 2H, CH₂); ^{13}C NMR (100 MHz, DMSO , δ , ppm): 166.5, 163.5, 161.2, 160.8, 159.9, 150.4, 147.6 (=CH), 140.7, 134.3, 132.72, 132.66, 130.50, 130.41, 130.0, 128.7, 128.3, 125.9, 125.7, 125.1, 123.2, 121.4, 119.4, 116.1, 115.9, 115.2, 45.7; LCMS (m/z): 474.5 (M+H)⁺; Anal. Calcd. For $\text{C}_{26}\text{H}_{17}\text{F}_2\text{N}_3\text{O}_2\text{S}$: C, 65.95; H, 3.62; N, 8.87. Found: C, 65.90; H, 3.70; N, 8.81.

3-(Z-(Z-3-(4-fluorophenyl)-4-oxo-2-(phenylimino)thiazolidin-5-ylidene)methyl)-6-chloro-quinolin-2(1H)-one (8 l)

Yield: 75%; FTIR (KBr, cm^{-1}): 3218, 3068, 2971, 1714, 1662, 1592; ^1H NMR (400 MHz, DMSO-d_6 , δ , ppm): 12.16 (s, 1H, -NH); 8.04 (s, 1H, Q-H₄); 7.92 (s, 1H, H₅), 7.85 (s, 1H, HC=); 7.61 (d, 1H, 8.4 Hz, Q-H₇); 7.51 (t, 1H, 6.8 Hz, Ar-H_{o,p}), 7.39–7.45 (m, 2H, 7.6 Hz, Ar-H); 7.33 (d, 1H, 8 Hz, Q-H₈); 7.21–7.28 (m, 3H, Ar-H); 7.00 (d, 2H, 8 Hz, Ar-H), 5.09 (s, 2H, -CH₂); ^{13}C NMR (100 MHz, DMSO , δ , ppm): 166.6, 163.2, 161.0, 160.0, 151.0, 148.0 (=CH), 140.2, 134.5, 133.1, 132.70, 132.64, 130.54, 130.45, 129.9, 128.5, 127.0, 126.0, 125.8, 125.4, 123.5, 121.1, 120.0, 117.0, 116.0, 115.8, 45.5; LCMS (m/z): 491.1 (M+H)⁺; Anal. Calcd. For $\text{C}_{26}\text{H}_{17}\text{ClFN}_3\text{O}_2\text{S}$: C, 63.74; H, 3.50; N, 8.58. Found: C, 63.84; H, 3.46; N, 8.62.

3-(Z-(Z-3-(4-fluorophenyl)-4-oxo-2-(phenylimino)thiazolidin-5-ylidene)methyl)-6-bromo-quinolin-2(1H)-one (8m)

Yield: 78%; FTIR (KBr, cm^{-1}): 3225, 3068, 2970, 1718, 1659, 1588; ^1H NMR (400 MHz, DMSO- d_6 , δ , ppm): 12.15 (s, 1H, -NH); 8.08 (s, 1H, Q- H_4); 8.00 (s, 1H, Q- H_5); 7.82 (s, 1H, HC=); 7.66 (d, 1H, 8.4 Hz, Q- H_8); 7.39–7.47 (m, 4H, Ar-H); 7.30 (d, 1H, 7.6 Hz, Q- H_7), 7.18–7.25 (m, 3H, Ar-H); 7.02 (d, 2H, 8 Hz, Ar-H), 5.08 (s, 2H, - CH_2); ^{13}C NMR (100 MHz, DMSO, δ , ppm): 166.5, 163.3, 160.0, 150.8, 148.3 (=CH), 140.0, 137.2, 134.1, 132.74, 132.69, 131.9, 130.58, 130.50, 130.0, 128.8, 126.0, 125.7, 125.3, 123.2, 121.3, 120.2, 116.6, 116.2, 116.0, 45.6; LCMS (m/z): 534.3 (M + H) $^+$; Anal. Calcd. For $\text{C}_{26}\text{H}_{17}\text{BrFN}_3\text{O}_2\text{S}$: C, 58.44; H, 3.21; N, 7.86. Found: C, 58.40; H, 3.25; N, 7.82.

3-(Z-(Z-3-(4-fluorophenyl)-4-oxo-2-(phenylimino)thiazolidin-5-ylidene)methyl)-6-methyl-quinolin-2(1H)-one (8n)

Yield: 80%; FTIR (KBr, cm^{-1}): 3209, 3068, 2975, 1714, 1660, 1595; ^1H NMR (400 MHz, DMSO- d_6 , δ , ppm): 12.02 (s, 1H, -NH); 8.01 (s, 1H, Q- H_4); 7.85 (s, 1H, HC=); 7.56 (s, 1H, Q- H_5); 7.51 (t, 2H, 6.4 Hz, Ar- $\text{H}_{\text{O-F}}$), 7.45 (t, 2H, Ar-H); 7.33 (d, 1H, 8 Hz, Q- H_7); 7.19–7.25 (m, 4H, Ar-H); 7.00 (d, 2H, 8 Hz, Ar-H), 5.09 (s, 2H, - CH_2); 2.32 (s, 3H, - CH_3); ^{13}C NMR (100 MHz, DMSO, δ , ppm): 166.5, 163.4, 161.1, 160.7, 150.2, 147.7 (=CH), 141.0, 137.7, 136.4, 134.2, 132.80, 132.74, 130.55, 130.47, 129.9, 128.5, 126.0, 125.8, 125.4, 123.5, 121.6, 120.0, 116.0, 115.8, 115.2, 45.8, 31.0; LCMS (m/z): 470.5 (M + H) $^+$; Anal. Calcd. For $\text{C}_{27}\text{H}_{20}\text{FN}_3\text{O}_2\text{S}$: C, 69.07; H, 4.29; N, 8.95. Found: C, 69.13; H, 4.25; N, 8.91.

3-(Z-(Z-3-(4-fluorophenyl)-4-oxo-2-(phenylimino)thiazolidin-5-ylidene)methyl)-6-methoxyquinolin-2(1H)-one (8o)

Yield: 76%; FTIR (KBr, cm^{-1}): 3219, 3063, 2972, 1718, 1663, 1591; ^1H NMR (400 MHz, DMSO- d_6 , δ , ppm): 12.00 (s, 1H, -NH); 7.99 (s, 1H, Q- H_4); 7.87 (s, 1H, HC=); 7.49 (t, 2H, Ar- $\text{H}_{\text{O-F}}$); 7.41 (t, 2H, 7.4 Hz, 7.4 Hz), 7.32 (s, 1H, Q- H_5); 7.20–7.26 (m, 5H, Ar-H); 7.01 (d, 2H, 8 Hz, Ar-H), 5.08 (s, 2H, - CH_2); 3.77 (s, 3H, - OCH_3); ^{13}C NMR (100 MHz, DMSO, δ , ppm): 166.3, 163.3, 160.9, 160.5, 155.0, 150.4, 147.9 (=CH), 140.7, 134.0, 132.82, 132.79, 130.57, 130.49, 130.0, 126.1, 126.0, 125.3, 123.2, 122.3, 121.5, 120.0, 117.0, 115.9, 115.7, 110.1, 56.0, 45.5; LCMS (m/z): 486.3 (M + H) $^+$; Anal. Calcd. For $\text{C}_{27}\text{H}_{20}\text{FN}_3\text{O}_3\text{S}$: C, 66.79; H, 4.15; N, 8.65. Found: C, 66.84; H, 4.21; N, 8.60.

Crystal structure solving procedure

A light yellow coloured rectangle-shaped single crystal of dimensions $0.28 \times 0.26 \times 0.23$ mm of the title compound was chosen for an X-ray diffraction study. The X-ray intensity data were collected at a temperature of 296 K on a Bruker Proteum2 CCD diffractometer equipped with an X-ray generator operating at 45 kV and 10 mA, using $\text{CuK}\alpha$ radiation of wavelength 1.54178 Å. Data were collected for 24 frames per set with different settings of ϕ (0° and 90°), keeping the scan width of 0.5° , exposure time of 2 s, the sample to detector distance of 45.10 mm and 2θ value at 46.6° . A complete data set was processed using SAINT PLUS [39]. The structure was solved by direct methods and refined by full-matrix least squares method on F^2 using SHELXS and SHELXL programmes [40]. All the non-hydrogen atoms were revealed in the first difference Fourier map itself. All the hydrogen atoms were positioned geometrically and refined using a riding model. After several cycles of refinement, the final difference Fourier map showed peaks of no chemical significance and the residuals saturated to 0.0965. The geometrical calculations were carried out using the programme PLATON [41]. The molecular and packing diagrams were generated using the software MERCURY [42].

Anticancer activity (MTT assay)

MDA-MB-231 cell culture was procured from National Centre for Cell Sciences (NCCS), Pune, India. The cells were cultured in Dulbecco's minimum essential medium (DMEM) supplemented with 10% Foetal bovine serum (FBS), Penicillin (100 IU/ml), Streptomycin (100 $\mu\text{g}/\text{ml}$) and Amphotericin-B (5 $\mu\text{g}/\text{ml}$) in a humidified atmosphere of 5% CO_2 at 37°C until confluent. The cells were trypsinized with Trypsin-EDTA solution. The stock cultures were grown in 25 cm^2 flasks and the studies were carried out in 96-well microtitre plates.

The cytotoxicity activity was done by MTT assay [43, 44] Cells were plated in 96-well flat-bottom microtitre plate at a density of 5×10^3 cells per well and cultured for 24 h at 37°C in 5% CO_2 atmosphere to allow cell adhesion. After 24 h, when partial monolayer was formed, medium was removed and cells were treated with different concentration of standard drug (cisplatin) and sample compounds for 48 h. After the treatment, the solutions in the wells were discarded and 100 μl of freshly prepared MTT (1 mg/ml, prepared in PBS) was added to each well. The plates were shaken gently and incubated for 4 h at 37°C in 5% CO_2 atmosphere. After 4 h, the supernatant was removed and the formazan crystals formed in the cells were solubilized by addition of 100 μl of

DMSO. Finally, the absorbance was read using a Micro-plate reader a wavelength of 540 nm.

The percentage growth was calculated using the formula below:

$$\% \text{ growth inhibition} = \frac{\text{control absorbance} - \text{test absorbance}}{\text{control absorbance}} \times 100.$$

From curve IC_{50} , (Concentration of drug required to kill 50% of cells in exponentially growing cultures after a 48 h exposure to the drug) values were calculated. The assay was conducted in triplicate.

Cytotoxicity on normal HEK 293 kidney cell line

Human embryonic kidney cell line HEK 293 was procured from NCCS, Pune. The cytotoxicity effects of **8e**, **8k**, **8m**, **8n** and **8o** were studied by MTT assay. The cells were cultured using Eagle's minimum essential medium (MEM) supplemented with 10% foetal bovine serum, penicillin (100 U mL⁻¹) and streptomycin (100 mg mL⁻¹) and grown in 25 cm² tissue culture flasks at 37 °C with 5% CO₂ incubator (Galaxy 170S, New Brunswick). After attaining 70–80% confluence, cells were trypsinized and seeded to 96-well plates in 100 mL of MEM (5000 cells/well). After 24 h, different concentrations of drugs were dissolved in DMSO are added to 96-well plates and incubated for 24 h at standard condition. Untreated cells represented a control group. Four replicates were set up for each test group. After completion of the incubation time, 20 mL of MTT dye (5 mg mL⁻¹ in PBS) was added to all wells; the plate was sealed with aluminium foil and incubated for 4 h in an incubator. After 4 h, 100 mL of DMSO was added to all the wells and mixed by uniform shaking. Using a multi-plate reader (LisaScan@EM), the absorbance was recorded at 570 nm.

The percentage growth inhibition was calculated using the formula below:

$$\% \text{ growth inhibition} = \frac{\text{control absorbance} - \text{test absorbance}}{\text{control absorbance}} \times 100.$$

From curve IC_{50} (Concentration of drug required to kill 50% of cells in exponentially growing cultures after a 48 h exposure to the drug) values were calculated. The assay was conducted in triplicate.

Cell cycle analysis

The compound **8n** was examined for its effects on the cell growth cycle [45]. After 24 h of serum starvation, MDA-MB-231 cells were treated with drug concentration 8.16 μM containing complete medium. The cells were harvested after 48 h and then spun at 1000 × *g* for 5 min. The supernatant was aspirated and the cell pellet was washed

with 1 × PBS. It was re-centrifuged and fixed in 70% cold EtOH for overnight fixation at 4 °C. After centrifugation, the cells were washed twice with ice-cold PBS and the pellet re-suspended in 200 μl of 1 × PBS mixture containing 0.1% Triton X-100, 100 μg/ml RNase and 10 μg/ml PI solution. The cells were incubated in the dark for 30 min at 4 °C and then analyzed by flow cytometry using MACS Quant Analyser. The distribution of cells in G₀/G₁, S, G₂/M phase was determined. Untreated cells harvested at the same time point served as control.

Molecular docking methods

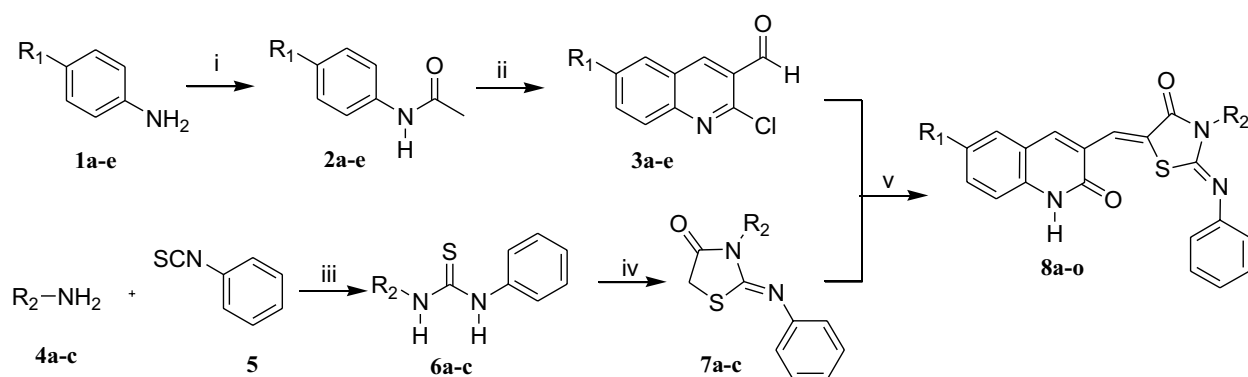
The docking studies and molecular dynamic simulation studies of Quinolono-thiazolidinone derivatives with hNAT-1 were performed by using Schrodinger Glide software as described in the literature [46].

Results and discussion

Synthesis

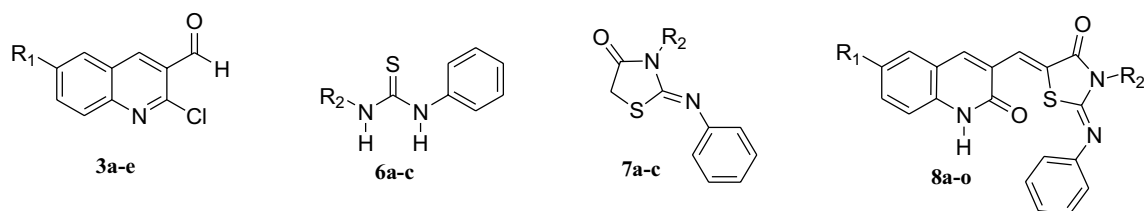
The synthetic route adapted for the preparation of 2-chloroquinoline-3-aldehydes **3a-e** and final compounds **8a-o** is depicted in Scheme 1. The quinoline-3-aldehydes **3a-e** were prepared by a well-known Meth-Cohn synthetic route [47]. Different anilines **1a-e** were reacted with acetic anhydride in THF medium to obtain corresponding acetanilides **2a-e** which on Vilsmeier-Haack formylation reaction with DMF-POCl₃ yielded 2-chloroquinoline-3-carboxaldehydes **3a-e**. In another route, different aliphatic/benzylamines **4a-c** were made to react with phenylisothiocyanate **5** in dimethylformamide solvent in the presence of triethylamine to generate 1-(alkyl/benzyl)-3-phenylthiourea **6a-c**. These were then cyclised with chloroacetic acid in sodium acetate to yield 3-(alkyl/benzyl)-2-(phenylamino)thiazolidin-4-ones **7a-c**. In the final step, target compounds **8a-o** were obtained by the Knoevenagel condensation of these thiazolidin-4-ones with different 2-chloro-6-substituted quinoline-3-carboxaldehyde **3a-e** in acetic acid-sodium acetate buffer medium. As we utilized acetic acid-sodium acetate solvent medium, the chlorine atom at 2nd position of quinoline ring underwent nucleophilic substitution reaction yielding quinolin-2-one derived products **8a-o**. Characterization data of all synthesized compound is presented in Table 1.

All the newly synthesized compounds were characterized by IR, ¹H NMR, ¹³C NMR, LCMS and elemental analysis. Formation of 1-(4-fluorobenzyl)-3-phenylthiourea **6c** was



Scheme 1: (i) Ac_2O , THF, rt (ii) DMF- POCl_3 , Reflux, 6 h (iii) TEA, DMF, rt (iv) Chloroacetic acid, sodium acetate, ethanol, reflux (v) NaOAc, glac. AcOH, reflux

Table 1 Characterization data of compounds **3a-e**, **6a-c**, **7a-c** and **8a-o**



Compd	R_1	R_2	M.p ($^\circ\text{C}$)
3a	F	–	68–70 [48]
3b	Cl	–	248–250 [49]
3c	Br	–	250–252 [48]
3d	Me	–	242–244 [48]
3e	OMe	–	244–246 [48]
6a	–	$-\text{CH}_2-\text{CH}_2-\text{CH}_3$	60–62 [50]
6b	–	$-\text{CH}_2-\text{C}_6\text{H}_5$	155–157 [51]
6c	–	$-\text{CH}_2-4\text{-F-C}_6\text{H}_4$	72–74 [50]
7a	–	$-\text{CH}_2-\text{CH}_2-\text{CH}_3$	55–57 [52]
7b	–	$-\text{CH}_2-\text{C}_6\text{H}_5$	66–68
7c	–	$-\text{CH}_2-4\text{-F-C}_6\text{H}_4$	68–70
8a	F	$-\text{CH}_2-\text{CH}_2-\text{CH}_3$	> 270
8b	Cl	$-\text{CH}_2-\text{CH}_2-\text{CH}_3$	> 270
8c	Br	$-\text{CH}_2-\text{CH}_2-\text{CH}_3$	258–260
8d	Me	$-\text{CH}_2-\text{CH}_2-\text{CH}_3$	> 270
8e	OMe	$-\text{CH}_2-\text{CH}_2-\text{CH}_3$	> 270
8f	F	$-\text{CH}_2-\text{C}_6\text{H}_5$	> 270
8g	Cl	$-\text{CH}_2-\text{C}_6\text{H}_5$	> 270
8h	Br	$-\text{CH}_2-\text{C}_6\text{H}_5$	> 270
8i	Me	$-\text{CH}_2-\text{C}_6\text{H}_5$	256–258
8j	OMe	$-\text{CH}_2-\text{C}_6\text{H}_5$	232–234
8k	F	$-\text{CH}_2-4\text{-F-C}_6\text{H}_4$	250–252
8l	Cl	$-\text{CH}_2-4\text{-F-C}_6\text{H}_4$	256–258
8m	Br	$-\text{CH}_2-4\text{-F-C}_6\text{H}_4$	> 270
8n	Me	$-\text{CH}_2-4\text{-F-C}_6\text{H}_4$	> 270
8o	OMe	$-\text{CH}_2-4\text{-F-C}_6\text{H}_4$	246–248

confirmed by its IR spectrum which showed two prominent peak at 3391 cm^{-1} and 3120 cm^{-1} for N–H stretching and at 1184 cm^{-1} for C=S stretching. Appearance of two distinct broad singlets at 9.64 ppm and 8.18 ppm in its ^1H NMR spectra for two N-H protons and its ^{13}C spectra showed a downfield signal at 181.2 ppm corresponding to C=S carbon confirms its formation. In the IR spectra of (Z)-3-(4-fluorobenzyl)-2-(phenylimino)thiazolidin-4-one **7c** absence of NH stretching bands and appearance new band at 1717 cm^{-1} corresponding to C=O stretching clearly confirms its cyclization from **6c**. In ^1H NMR spectra, cyclization to **7c** was evidenced by the emergence of a sharp singlet at 4.10 ppm corresponding to –S–CH₂ proton with the disappearance of two broad NH peaks. Its ^{13}C NMR spectra showed signals at 172.4 ppm and 155.4 ppm corresponding to the ring carbonyl (C=O) carbon and C=N, respectively, confirming the formation. Its LCMS spectrum showed a (M+H) peak at 301.1 confirming its formation.

The Knoevenagel condensation between different substituted quinoline aldehydes **3a–e** and substituted thiazolidinone **7a–c** yielded the final compounds **8a–o**. In the IR spectra of **8a**, appearance of a peak at 3150 cm^{-1} for the NH stretching confirms the nucleophilic displacement of chlorine in the presence of glacial acetic acid to form NH–C=O. Moreover, appearance two distinct carbonyl peaks at 1697 cm^{-1} and 1655 cm^{-1} corresponding to ring carbonyl and ring NH–C=O confirms its formation. The nucleophilic displacement of chlorine is due to the presence of water molecule in the reaction medium

that is eliminated during the condensation process. The ^1H NMR spectrum of compounds **8a–o** showed exocyclic =C–H singlet in the region 7.70–7.90 ppm which confirms the Knoevenagel condensation products. In the ^1H NMR spectrum of compound **8o**, a broad peak at 12.00 ppm for N–H confirms the nucleophilic displacement reaction. The methoxy protons appeared at 3.77 ppm and CH₂ protons at 5.08 ppm as two distinct singlets. The exocyclic =CH proton resonated as a singlet at 7.87 ppm. Further, ^{13}C NMR spectra of **8o**, a peak corresponding to C=O carbon appeared at 166.3 ppm and a peak at 160.5 ppm corresponding to C=O carbon of quinoline NH–C=O confirms the product. Also, the exocyclic methine proton resonated at 147.9 ppm confirming its formation. The signals corresponding to the carbons of 4-fluoro phenyl ring exhibited splitting due to the presence of fluorine atom. The carbon attached to the fluorine atom displayed a doublet at 163.27 and 160.85 ppm with coupling constant 242 Hz and ortho carbon appeared as doublet with coupling constant of 21 Hz at 115.93 and 115.72 ppm. Meta and para carbons appeared as doublets at 130.57, 130.49 ppm and 132.82, 132.79 ppm with coupling constants 8 Hz and 3 Hz, respectively. The coupling constant clearly distinguishes the different carbon atoms.

Crystal structure of **8a**

The Z-configuration of exocyclic C=C and C=N was confirmed by the crystal structure of **8a** (Fig. 2). The details of

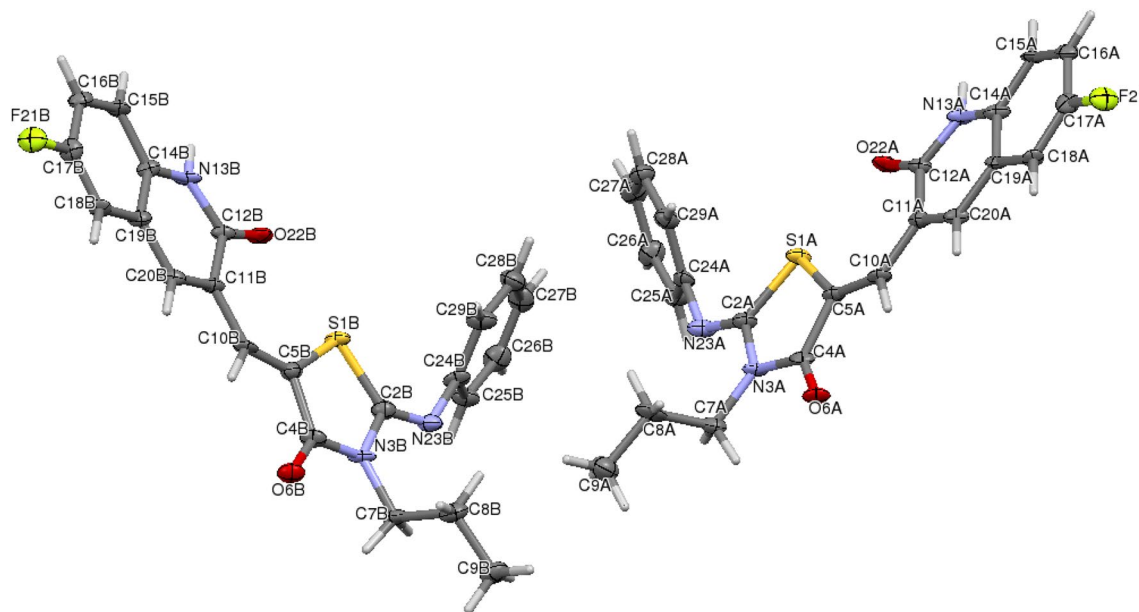


Fig. 2 ORTEP diagram of **8a**

Table 2 Crystal refinement data of **8a**

Parameter	Value
CCDC deposit No	1437323
Empirical formula	C ₄₄ H ₃₆ F ₂ N ₆ O ₄ S ₂
Formula weight	814.91
Temperature	293(2) K
Wavelength	1.54178 Å
Crystal system, space group	Triclinic, <i>P</i> -1
Unit cell dimensions	<i>a</i> = 6.5527(5) Å <i>b</i> = 10.4546(8) Å <i>c</i> = 29.118(2) Å α = 97.984(5) ^o β = 91.684(5) ^o γ = 106.584(5) ^o
Volume	1888.2(3) Å ³
Z, Calculated density	2, 1.433 Mg/m ³
Absorption coefficient	1.819 mm ⁻¹
<i>F</i> ₍₀₀₀₎	848
Crystal size	0.28 × 0.26 × 0.23 mm
Theta range for data collection	1.54 ^o to 58.93 ^o
Limiting indices	-7 ≤ <i>h</i> ≤ 6, -11 ≤ <i>k</i> ≤ 11, -32 ≤ <i>l</i> ≤ 32
Reflections collected/unique	26,164/ 5370 [R(int)=0.0972]
Refinement method	Full-matrix least-squares on <i>F</i> ²
Data/restraints/parameters	5370/0/525
Goodness-of-fit on <i>F</i> ²	1.231
Final R indices [<i>I</i> > 2σ(<i>I</i>)]	<i>R</i> 1 = 0.0965, <i>wR</i> 2 = 0.2482
R indices (all data)	<i>R</i> 1 = 0.1127, <i>wR</i> 2 = 0.2554
Largest diff. peak and hole	0.581 and -0.467 e. Å ⁻³

the crystal structure and data refinement are given in Table 2. The compound **8a** crystallizes in the triclinic space group *P*-1 with two independent molecules in the asymmetric unit. The C5–C10 and N23–C2 bonds in both the molecules of A and B shows a typical double-bond character corresponding to ethene and imine bonds, with bond lengths 1.336(1) Å (C5A–C10A), 1.334(1) Å (C5B–C10B) and 1.278(10) Å (N23A–C2A), 1.268(10) Å (N23B–C2B) respectively. The C10–C11 bond shows a partial double-bond character, with the bond lengths 1.461(11) Å (C10A–C11A) and 1.467(10) Å (C10B–C11B), respectively, which seems to indicate a certain electronic delocalization between C5–C10 and C10–C11 bonds in both the molecules. The double bonds C5–C10 and N23–C2 adopts a *Z,Z* configuration in both the molecules which is in agreement with the reported literature molecules [23, 53]. The central thiazolidinone ring is planar and keeps the planarity across the ethene bond with the quinoline moiety. The dihedral angle between the central thiazolidinone ring and the quinoline ring bridged by the ethene bond is 54.0(4)^o (S1A–C5A & C24A–C29A), 54.8(4)^o (S1B–C5B & C24B–C29B), respectively, whereas the dihedral angle between the thiazolidinone ring and the fused heterocyclic

Table 3 Anticancer activity of compounds **8a-o**

Comp	IC ₅₀ (μM)		
	MDA-MB-231	MCF-7	HEK-293
8a	> 100	NT	NT
8b	> 100	NT	NT
8c	46.09	NT	NT
8d	27.61	NT	NT
8e	17.68	39.38	> 1000
8f	59.32	NT	NT
8g	46.11	NT	NT
8h	> 100	NT	NT
8i	33.77	NT	NT
8j	39.99	NT	NT
8k	22.20	36.98	682.12
8l	> 100	NT	NT
8m	18.75	24.72	> 1000
8n	8.16	33.86	846.93
8o	44.24	18.03	409.72
Cisplatin	1.66	4.99	NT

ring bridged by the imine bond is 10.0(3)^o (S1A–C5A & C11A–C20A), 10.5(3)^o (S1B–C5B & C11B–C20B) respectively. The crystal structure is stabilized by both inter and intramolecular hydrogen bonds of the type N–H...O and C–H...O.

Anticancer activity

All the target compounds **8a-o** were tested for their anticancer activity against MDA-MB-231 human breast cancer cell line and five potent compound against MCF-7 cell lines by MTT assay. The anticancer data are depicted in Table 3. Compound **8n** having methyl substitution at the 6th position of quinolone and 4-fluorophenyl moiety at the 3rd position of thiazolidinone ring exhibited the excellent activity in the series with IC₅₀ 8.16 μM against MDA-MB-231 cell line but moderate activity against MCF-7 with IC₅₀ 33.86 μM. Next best activity was exhibited by compound **8e** which has a methoxy substitution at the 6th position of quinolone with propyl group at the 3rd position of thiazolidinone ring showed IC₅₀ 17.68 μM against MDA-MB-231 cell line and 39.38 μM on MCF-7 cell line. Compound **8m** showed good activity with IC₅₀ 18.75 μM on MDA-MB-231 cell line and a slightly reduced activity with IC₅₀ value of 24.72 μM against MCF-7 cell line. Compounds **8k** having fluorine group at the 6th position exhibited good activity against MDA-MB-231 cell line with IC₅₀ 22.20 μM and **8o** having methoxy group showed moderate activity IC₅₀ 44.24 μM on MDA-MB-231, but it showed promising activity against MCF-7 cell line with IC₅₀ 18.03 μM. The compounds from propyl series **8c** (6-Br) and **8d** (6-Me) were found to be

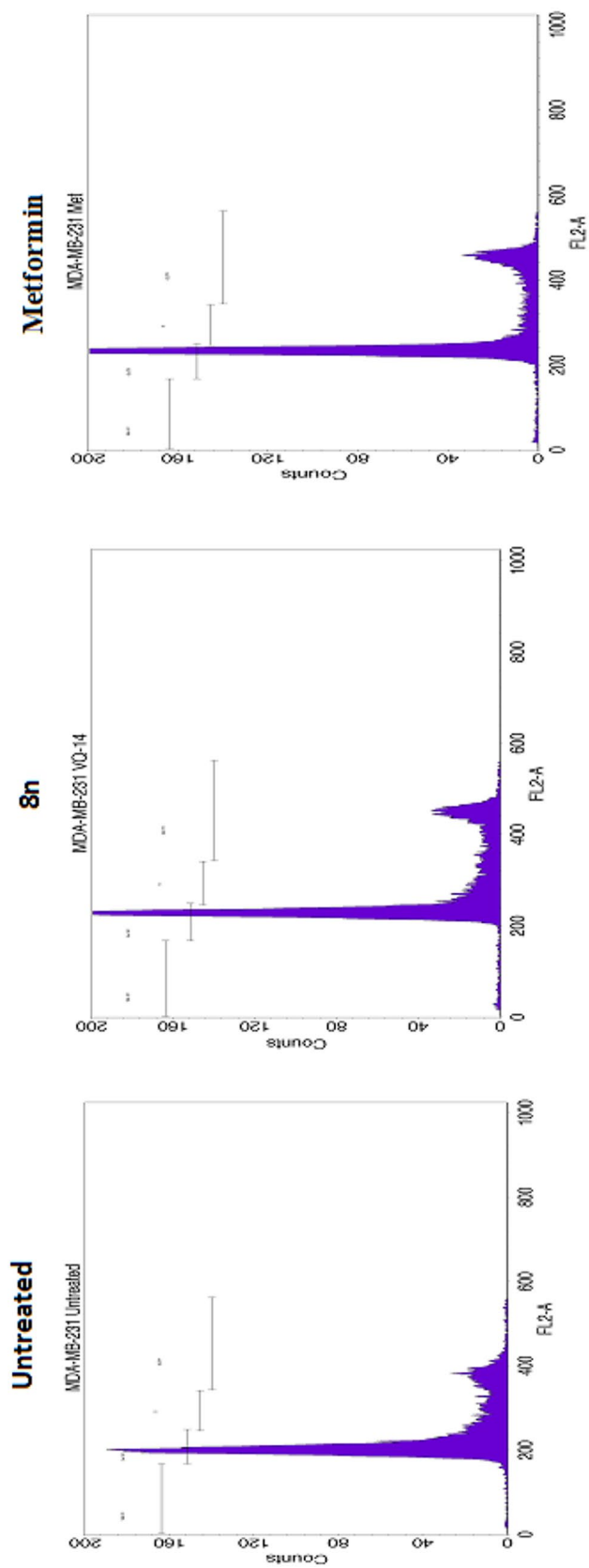


Fig. 3 Cell cycle analysis data on MDA-MB-231 cell line for untreated group, **8n** and Metformin

Table 4 Cell cycle analysis of **8n** on MDA-MB-231 cell line

Phases	Untreated	8n ^a	Metformin ^b
G ₀ /G ₁	56.59	50.52	57.76
S	12.09	15.66	12.38
G ₂ /M	11.20	19.73	18.45
Sub G ₁	0.84	1.21	1.07

^a experiment carried out at 8.16 μ M concentration (IC₅₀)^b experiment carried out at 20 μ M concentration

moderate inhibitors with IC₅₀ 46.09 and 27.61 μ M respectively. Benzylic series compounds exhibited moderate activity against MDA-MB-231 cell line with IC₅₀ 33.77 μ M and 39.99 μ M for **8i** (6-Me) and **8j** (6-OMe) respectively. Moreover, compounds **8f** from the same series displayed very less activity with IC₅₀ 59.32 μ M.

Toxicity study on normal HEK-293 cell line

Toxicity profile of potent compounds **8e**, **8k**, **8m**, **8n** and **8o** was determined by MTT assay on normal human kidney HEK 293 cell line and results are given in Table 3. From the study, it was clear that all the tested compounds were found to be non-toxic and safer to normal cell line even at higher concentrations.

Cell cycle analysis of **8n**

In order to determine the mode of action of potent compound **8n**, cell cycle analysis was performed at its IC₅₀ concentration 8.16 μ M in MDA-MB-231 cell line using Flow cytometry method (Fig. 3 and Table 4). It was observed that 19.73% of cells were accumulated at the G₂/M phase as compared to the control which has 11.20% of cells. Similarly, standard drug Metformin has 18.45% of cells in G₂/M phase. At the same time there is a slight increase in the cell counts in the S phase when compared to control cells. However, there is no considerable distribution of cells among the different phases

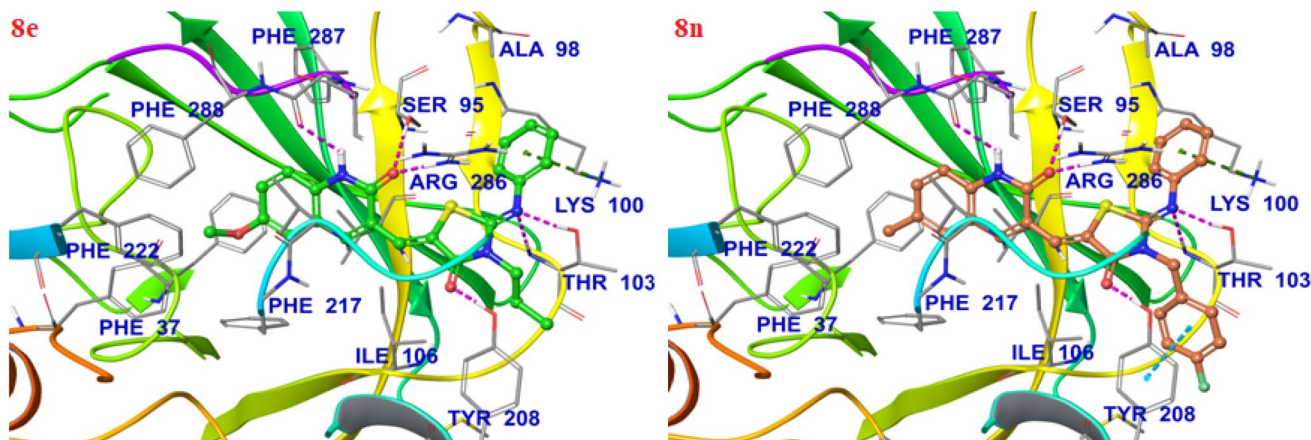


Fig. 4 Docking pose of compound **8e** and **8n** with human NAT-1. The violet colour dotted lines represent hydrogen bonding, cyan colour lines represents π - π interaction and blue colour dotted lines represents π -cation interactions

Table 5 Docking scores and interactions with NAT-1 protein for the compounds **8e** and **8n**

Compound	Docking score (kcal/mol)	Hydrogen bonding	π - π stacking and π -cation interactions	Hydrophobic interactions
8e	- 12.592	Phe287, Arg286, Ser95, Tyr208, Thr103	Arg286, Cys100	Ile106, Ala98, Tyr101, Val216, Phe288, Phe37, Phe125, Phe217, Leu209 and Val93
8n	- 14.678	Phe287, Arg286, Ser95, Tyr208, Thr103	Phe217, Arg286, Cys100, Tyr208	Ile106, Met205, Ala98, Tyr101, Val216, Phe288, Phe37, Phe125, Phe217, Leu209 and Val93

at the IC_{50} concentration. But with the observed accumulation of cells at 8.16 μ M concentration, compound **8n** was found to arrest the cell cycle at G_2/M phase.

Molecular docking studies

Selection of target protein

In order to determine the possible binding modes of potent compounds with the protein, docking studies were carried out on human *N*-acetyl transferase-1 protein (NAT-1) using Schrodinger molecular docking toolkit. The selection of target protein for the docking studies was done on the basis of structural similarity of reported molecules (Fig. 1). It was reported that 5-(2-hydroxybenzylidene)-2-thioxothiazolidin-4-one as NAT-1 inhibitor of breast cancer cells ZR-75-1 [34] and MDA-MB-231 [35]. Similarly, thiazolidine-2,4-diones [54] were reported as NAT inhibitors of mycobacterium tuberculosis. Our target compounds **8a-o** structurally mimic the reported NAT inhibitors and modification was done at the 2nd, 3rd and 4th position of central thiazolidinone. Hence, quinoline-thiazolidinones **8a-o** were docked on human *N*-acetyl transferase-1 protein by induced fit docking method.

Docking studies

The docking studies of quinazoline clubbed thiazolidinones with hNAT-1 protein (PDB: 2PQT) were carried out by using Schrödinger Glide [55] and the docking poses of compounds **8n** and **8e** are depicted in Fig. 4. The corresponding docking score and residual interaction are given in Table 5.

In the docking pose of compound **8n**, which has a docking score of -14.678 kcal/mol which exhibited strong hydrogen bonding interaction between N-H of quinolone with the backbone oxygen of Phe287 at a distance of 2.10 Å and carbonyl oxygen of quinolone interacted with the side chain amino group of Arg286 at a distance of 1.89 Å. Also, this carbonyl oxygen forms another hydrogen bond with hydroxyl group of Ser95 with a bond length of 1.97 Å. The thiazolidinone carbonyl oxygen also makes strong hydrogen bond interaction with the side chain hydroxyl group of Tyr208 with a bond length of 1.73 Å. The exocyclic imine nitrogen is involved in hydrogen bonding with the main chain amino group of Thr103 at a distance of 2.01 Å and it also exhibits side chain interaction with hydroxyl group of Thr103 at a distance of 2.24 Å. The phenyl ring of quinolone moiety is involved in a strong π - π stacking moiety with Phe-217. Also phenyl ring at the 2nd position of thiazolidinone involved in the salt bridge with Arg286 and Lys100. In addition, it was stabilized by a π - π stacking interaction between phenyl ring of 4-fluoro moiety and Tyr208. The molecule oriented in hydrophobic cavity surrounded by Ile106, Met205, Ala98,

Tyr101, Val216, Phe288, Phe37, Phe125, Phe127, Leu209 and Val93 residues.

In the propyl series, the most potent compound **8e** has a docking score of -12.592 kcal/mol. Hydrogen bonding interaction present between N-H of quinoline with the main chain oxygen of Phe287 at a distance of 1.96 Å. Carbonyl oxygen of quinoline interacted with the side chain amino group of Arg286 at a distance of 1.76 Å and with hydroxyl group Ser95 with a bond length of 2.11 Å. The thiazolidinone carbonyl oxygen is involved in hydrogen bonding interaction with the side chain hydroxyl group of Tyr208 with a bond length of 1.73 Å. The exocyclic imine nitrogen forms binding with the main chain amino group of Thr103 at a distance of 2.02 Å. This molecule forms only two salt bridge interaction between the phenyl ring at the 2nd position of thiazolidinone with Arg286 and Lys100. The absence of two π - π stacking may accounts for its slightly lower activity. The residues Ile106, Ala98, Tyr101, Val216, Phe288, Phe37, Phe125, Phe127, Leu209 and Val93 forms hydrophobic interaction with the molecule.

Molecular dynamics simulations

Molecular dynamics (MD) simulation was performed to confirm the stability of predicted binding mode of the compounds to hNAT1. The molecular dynamics simulation was run using Desmond [56]. Simulation was run for 20 ns on equilibrated docked complex of **8n** with hNAT1 structures and at every 2 fs ensembles were saved in the trajectory. To evaluate the stability of the protein during dynamics, all the frames in the trajectory were aligned initial frame and the rmsd was calculated with respect to the initial frame. From 5 ns to till the end of simulation, the total rmsd of protein was within a range of 0.63 Å which depicted the protein was well stabilized during dynamics. Further, the rmsd observed for the ligand was within the range of 0.55 Å demonstrated the protein-ligand complex was well stabilized (Fig. 5).

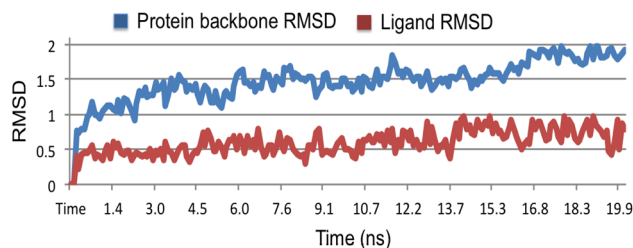


Fig. 5 The RSM deviations between the original structure and the structure enumerated during MD simulation; the backbone fluctuations are shown in blue, ligand fluctuations are shown in brown colour

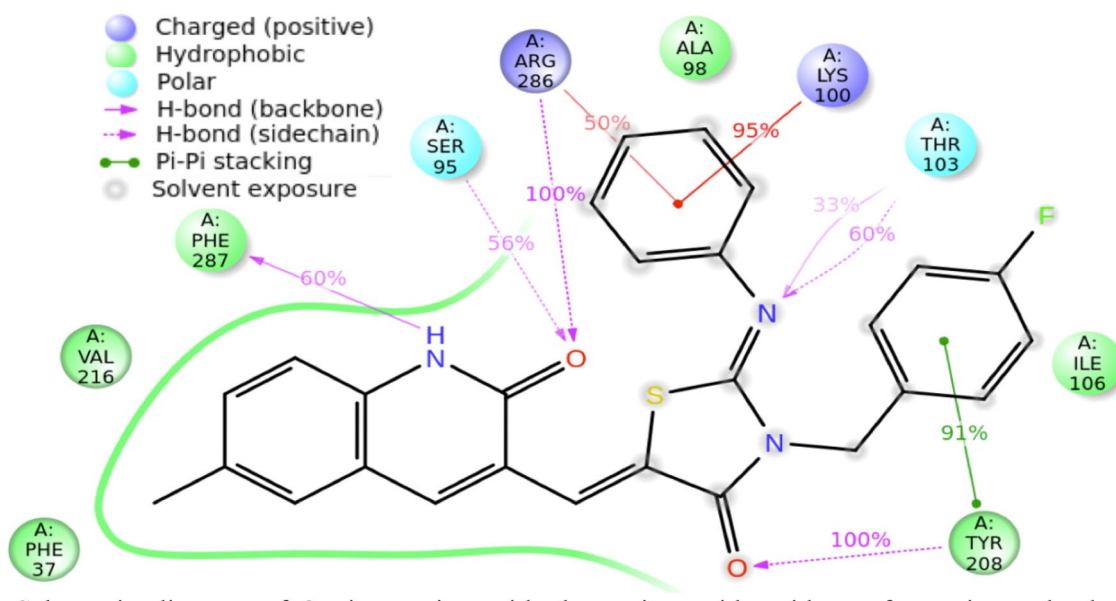
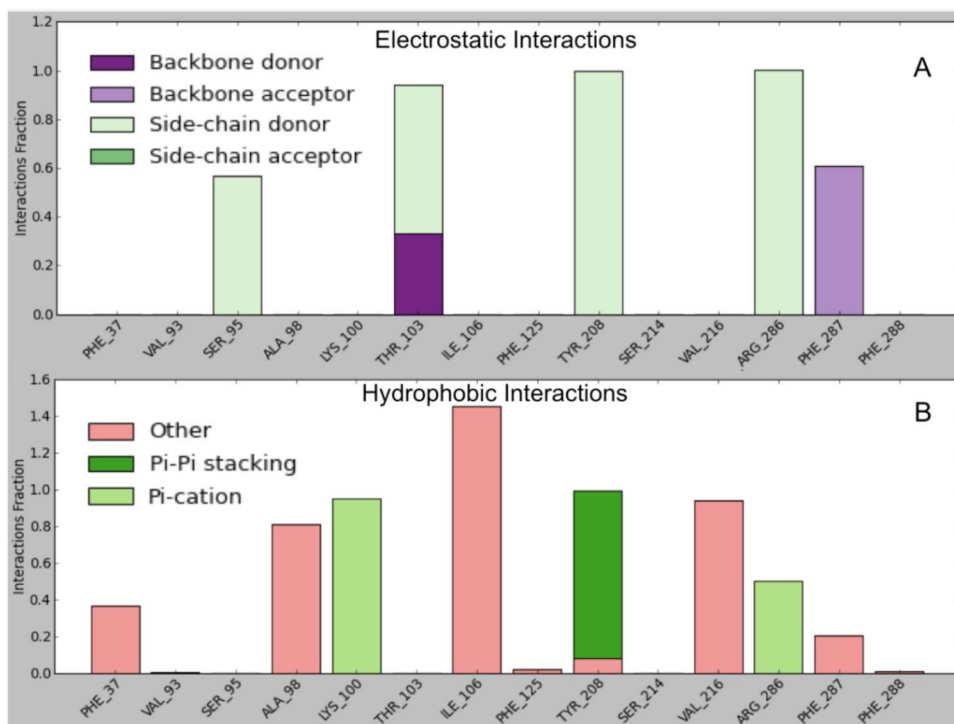


Fig. 6 Schematic diagram of **8n** interaction with the amino acid residues of protein evolved during MD simulation. Interactions that occur more than 30% of the simulation time are shown. Residues with the

ligand interactions that occurred more than 30% of the simulation time in the trajectory is shown

Fig. 7 Interaction between HNAT1 and **8n** evolved during MD simulation, A. depicts the electrostatic interactions and B. depicts the hydrophobic interactions



For the trajectory of the stable dynamics, the interactions between the protein and ligand were analysed. Figure 6 shows schematic diagram of the **8n** interacting with the amino acid residues of protein structure evolved during MD simulation. As illustrated in the figure, the ligand–protein interactions obtained in the docking study were conserved

throughout the MD simulation. The interactions obtained from the trajectory shows that major interactions between the ligand and receptor binding site amino acids are H-bond and hydrophobic (Fig. 7). As illustrated in the Fig. 7, H-bond amongst Phe287 and Ser95, hydrophobic interactions amongst Phe37, Val93, Ile106, Phe125, Val216, Phe217,

Phe222 and Phe288 with quinolinone moiety, H-bond amongst Tyr208 and Thr103 with 2-iminothiazolidin-4-one moiety, π -cation interaction amongst Arg286 and Lys100 with phenyl moiety and π - π stacking interaction amongst Tyr208 with fluoro-benzyl moiety were elegant in stabilizing the ligand in protein binding pocket.

Conclusion

In the present study, we synthesized few newer hybrid molecules containing quinolone and thiazolidinone moieties and evaluated their anticancer activities against two breast cancer cell lines MDA-MB-231 and MCF-7. All the compounds are characterized by spectroscopic techniques and E/Z-configurations of final molecules are confirmed by the crystal structure data of **8a**. It indicated that both the exocyclic C=N bond and C=C bond are in Z-configuration with respect to thiazolidinone ring. Few of the compounds exhibited good to moderate anticancer activity. Compound **8n** exhibited the promising activity against MDA-MB-231 cell line with IC₅₀ 8.16 μ M and compound **8o** showed potent activity on MCF-7 cancer cell line with IC₅₀ 18.03 μ M. Compound **8n** found to be non-toxic to the normal human kidney cell line. It has arrested the cell cycle at G₂/M phase of MDA-MB-231 cell line at its IC₅₀ concentration. SAR studies demonstrated that 4-fluoro phenyl ring and electron releasing groups in the quinolone moiety played major role in the enhancement of anticancer activity. Further, molecular docking studies exhibited that these compounds have well binding interactions with human N-acetyl transferase 1 protein having both hydrogen and π - π interactions.

Supporting information

Spectral data associated with this article are available in the supplementary material file.

Acknowledgements Authors are thankful to Yenepoya Research Centre, Yenepoya University, Deralakatte for helping in carryout anticancer activity. Also thankful to IOE and DST-PURSE, Vijnana Bhavana, University of Mysuru for X-ray crystallographic facility.

Declarations

Conflict of interest The authors declare that they have no conflict of interest.

References

1. L.A. Torre, F. Bray, R.L. Siegel, J. Ferlay, J. Lortet-Tieulent, A. Jemal, *CA Cancer J. Clin.* **65**, 87 (2015)
2. R. Siegel, J. Ma, Z. Zou, A. Jemal, *CA Cancer J. Clin.* **64**, 9 (2014)
3. K.M. El-Gamal, M.S. Hags, H.S. Abulkhair, *Bull. Fac. Pharm. Cairo Univ.* **54**, 263 (2016)
4. T.G. Shruthi, S. Eswaran, P. Shivarudraiah, S. Narayanan, S. Subramanian, *Bioorg. Med. Chem. Lett.* **29**, 97 (2019)
5. R.G. Kalkhambkar, G. Aridoss, G.M. Kulkarni, *Monatsh. Chem.* **143**, 1075 (2012)
6. M. Chioua, E. Martínez-Alonso, R. Gonzalo-Gobernado, M.I. Ayuso, A. Escobar-Peso, L. Infantes, D. Hadjipavlou-Litina, J.J. Montoya, J. Montaner, A. Alcázar, J. Marco-Contelles, *J. Med. Chem.* **62**, 2184 (2019)
7. Y. Zhang, Y. Fang, H. Liang, H. Wang, K. Hu, X. Liu, X. Yi, Y. Peng, *Bioorg. Med. Chem. Lett.* **23**, 107 (2013)
8. X.Q. Deng, M.X. Song, Y. Zheng, Z.S. Quan, *Eur. J. Med. Chem.* **73**, 217 (2014)
9. P.N. Batalha, M.C. Vieira de Souza, E. Peña-Cabrera, D.C. Cruz, F. da Costa Santos Boechat, *Curr. Pharm. Des.* **22**, 6009 (2016)
10. W.B. Kuang, R.Z. Huang, J.L. Qin, X. Lu, Q.P. Qin, B.Q. Zou, Z.F. Chen, H. Liang, Y. Zhang, *Eur. J. Med. Chem.* **157**, 139 (2018)
11. Y.C. Yu, W.B. Kuang, R.Z. Huang, Y.L. Fang, Y. Zhang, Z.F. Chen, X.L. Ma, *Med. Chem. Commun.* **8**, 1158 (2017)
12. S. Raghavan, P. Manogaran, K.K. Narasimha, B.K. Kuppusami, P. Mariyappan, A. Gopalakrishnan, G. Venkatraman, *Bioorg. Med. Chem. Lett.* **25**, 3601 (2015)
13. M.S. Kaur, R. Kaur, R. Bhatia, K. Kumar, V. Singh, R. Shankar, R. Kaur, R.K. Rawal, *Bioorg. Chem.* **75**, 406 (2017)
14. M. Kalhor, S. Banibairami, *RSC Adv.* **10**, 41410 (2020)
15. N. Azizi, M. Hasani, M. Khajeh, M. Edrisi, *Tetrahedron Lett.* **56**, 1189 (2015)
16. M.A. Ansari, D. Yadav, M.S. Singh, *J. Org. Chem.* **85**, 8320 (2020)
17. M. Fesatidou, P. Zagaliotis, C. Camoutsis, A. Petrou, P. Eleftheriou, C. Tratat, M. Haroun, A. Geronikaki, A. Ciric, M. Sokovic, *Bioorg. Med. Chem.* **26**, 4664 (2018)
18. M. Haroun, C. Tratat, A. Kolokotroni, A. Petrou, A. Geronikaki, M. Ivanov, M. Kostic, M. Sokovic, A. Carazo, P. Mladěnka, N. Sreeharsha, *Antibiotics.* **10**, 309 (2021)
19. Y. Ali, M.S. Alam, H. Hamid, A. Husain, A. Dhulap, S. Bano, C. Kharbanda, *Bioorg. Med. Chem. Lett.* **27**, 1017 (2017)
20. S.S. Abd El-Karim, H.S. Mohamed, M.F. Abdelhameed, A.E. Amr, A.A. Almehezia, E.S. Nossier, *Bioorg. Chem.* **111**, 104827 (2021)
21. R.N. Shelke, D.N. Pansare, A.P. Sarkate, K.S. Karnik, A.P. Sarkate, D.B. Shinde, S.R. Thopate, *J. Taibah Univ. Sci.* **13**, 678 (2019)
22. N. Trotsko, *Eur. J. Med. Chem.* **215**, 113266 (2021)
23. K.R.A. Abdellatif, W.A.A. Fadaly, G.M. Kamel, Y.A.M.M. Elshaier, M.A. El-Magd, *Bioorg. Chem.* **82**, 86 (2019)
24. A.D. Patel, T.Y. Pasha, P. Lunagariya, U. Shah, T. Bhambaroliya, R.K. Tripathi, *ChemMedChem* **15**, 1229 (2020)
25. M.F. Ansari, S.M. Siddiqui, K. Ahmad, F. Avecilla, S. Dharavath, S. Gourinath, A. Azam, *Eur. J. Med. Chem.* **124**, 393 (2016)
26. M.L. Barreca, A. Chimirri, L. De Luca, A.M. Monforte, P. Monforte, A. Rao, M. Zappalà, J. Balzarini, E. De Clercq, C. Pannecoque, M. Witvrouw, *Bioorg. Med. Chem. Lett.* **11**, 1793 (2001)
27. M. Mishchenko, S. Shtrygol, D. Kaminsky, R. Lesyk, *Sci. Pharm.* **88**, 16 (2020)

28. G. Çakir, İ Küçükgülzel, R. Guhamazumder, E. Tatar, D. Manvar, A. Basu, B.A. Patel, J. Zia, T.T. Talele, N. Kaushik-Basu, *Arch. Pharm. (Weinheim)*. **348**, 10 (2015)
29. D.K. Sigalapalli, V. Pooladanda, M. Kadagathur, S.D. Guggilapu, J.L. Uppu, C. Godugu, N.B. Bathini, N.D. Tangellamudi, *J. Mol. Struct.* **1225**, 128847 (2021)
30. M.A. Iqbal, A. Husain, O. Alam, S.A. Khan, A. Ahmad, M.R. Haider, M.A. Alam, *Arch. Pharm. (Weinheim)*. **353**, 2000071 (2020)
31. C.M. Richardson, C.L. Nunns, D.S. Williamson, M.J. Parratt, P. Dokurno, R. Howes, J. Borgognoni, M.J. Drysdale, H. Finch, R.E. Hubbard, P.S. Jackson, P. Kierstan, G. Lentzen, J.D. Moore, J.B. Murray, H. Simmonite, A.E. Surgenor, C.J. Torrance, *Bioorg. Med. Chem. Lett.* **17**, 3880 (2007)
32. M.F. Ansari, D. Idrees, M.I. Hassan, K. Ahmad, F. Avecilla, A. Azam, *Eur. J. Med. Chem.* **144**, 544 (2018)
33. H.H. Abdu-Allah, S.G. Abdel-Moty, R. El-Awady, A.N. El-Shorbaji, *Bioorg. Med. Chem. Lett.* **26**, 1647 (2016)
34. A.J. Russell, I.M. Westwood, M.H. Crawford, J. Robinson, A. Kawamura, C. Redfield, N. Laurieri, E.D. Lowe, S.G. Davies, E. Sim, *Bioorg. Med. Chem.* **17**, 905 (2009)
35. J.M. Tiang, N.J. Butcher, R.F. Minchin, *Biochem. Biophys. Res. Commun.* **393**, 95 (2010)
36. N. Raganathan, J. Dairou, B. Pluvinage, M. Martins, E. Petit, N. Janel, J.M. Dupret, F. Rodrigues-Lima, *Mol. Pharmacol.* **73**, 1761 (2008)
37. K.H. Lu, K.L. Lin, T.C. Hsia, C.F. Hung, M.C. Chou, Y.M. Hsiao, J.G. Chung, *Res. Commun. Mol. Pathol. Pharmacol.* **109**, 319 (2001)
38. J.H. Lee, H.F. Lu, D.Y. Wang, D.R. Chen, C.C. Su, Y.S. Chen, J.H. Yang, J.G. Chung, *Res. Commun. Mol. Pathol. Pharmacol.* **115–116**, 217 (2004)
39. Bruker, SAINT PLUS, Bruker AXS Inc., Madison, Wisconsin, USA, (2012)
40. G.M. Sheldrick, A short history of SHELX. *Acta Cryst.* **A64**, 112 (2008)
41. A.L. Spek, PLATON. *Acta Cryst.* **A46**, C34 (1990)
42. C.F. Macrae, I.J. Bruno, J.A. Chisholm, P.R. Edgington, P. McCabe, E. Pidcock, L. Rodriguez-Monge, R. Taylor, J. Van De Streek, P.A. Wood, *J. Appl. Cryst.* **41**, 466 (2008)
43. T.J. Mosmann, *Immunol. Methods.* **65**, 55 (1983)
44. F. Denizot, R. Lang, *Immunol. Methods.* **89**, 271 (1986)
45. X. Yang, W. Wang, J.J. Qin, M.H. Wang, H. Sharma, J.K. Buolamwini, H. Wang, R. Zhang, *PLoS ONE* **7**, e34303 (2012)
46. K.S.V. Kumar, G.S. Lingaraju, Y.K. Bommegowda, A.C. Vinayaka, P. Bhat, C.S.P. Kumara, K.S. Rangappa, D.C. Gowda, M.P. Sadashiva, *RSC Adv.* **5**, 90408 (2015)
47. O. Meth-Cohn, *Heterocycles* **35**, 539 (1993)
48. G.K. Nagaraja, G.K. Prakash, M.N. Kumaraswamy, V.P. Vaidya, K.M. Mahadevan, *ARKIVOC* **15**, 160 (2006)
49. A. Kedjadja, F. Moussaoui, A. Debache, S. Rhouati, A. Belfaitah, *J. Soc. Alger. Chim.* **14**, 225 (2004)
50. R. Ottana, R. Maccari, M.L. Barreca, G. Bruno, A. Rotondo, A. Rossi, G. Chiricosta, R. Di Paola, L. Sautebin, S. Cuzzocrea, M.G. Vigorita, *Bioorg. Med. Chem.* **13**, 4243 (2005)
51. P.V. Indukumari, C.P. Joshua, *Indian J. Chem. Section B: Organic Chemistry Including Medicinal Chemistry.* **19B**, 672 (1980)
52. T. Okawara, K. Nakayama, M. Furukawa, *Heterocycles* **19**, 1571 (1982)
53. F. Mushtaque, Md. Avecilla, Z.B. Hafeez, M.M.A. Rizvic, *J. Heterocycl. Chem.* **56**, 1794 (2019)
54. E.W. Brooke, S.G. Davies, A.W. Mulvaney, F. Pompeo, E. Sim, R.J. Vickers, *Bioorg. Med. Chem.* **11**, 1227 (2003)
55. Glide, version 6.7, Schrodinger, LLC, New York, NY, (2015)
56. Schrodinger release 2015–1: Desmond Molecular Dynamics System, version, 4.1, D.E. Shaw research, New York, NY. (2015)